Experimental investigation of oscillations in a magnetic nozzle

Davide Maddaloni, Jaume Navarro-Cavallé, Mario Merino, Filippo Terragni

Equipo de Propulsión Espacial y Plasmas (EP2), Universidad Carlos III de Madrid

Oscillations within the plume of a Helicon Plasma Thruster (HPT) prototype are experimentally collected, analyzed, and discussed. The data is gathered by means of an array of Langmuir probes displaced and experimental dispersion diagrams are recovered. Results show a different oscillatory behavior depending on the analyzed position and operating regime.

Magnetic nozzles

- Electric propulsion (EP) devices have several advantages over chemical propulsion
- Magnetic Nozzles are emerging as a new technology promising advantages over classical devices
  - Reduced erosion
  - Increased lifespan
  - Potential use of alternative propellants
- Examples of thrusters using magnetic nozzles are Helicon Plasma Thruster and Electron Cyclotron Resonance

Plasma oscillations

- Instabilities are nearly ubiquitous in plasma physics
  - Electric propulsion
  - Fusion reactors
  - Astrophysics
  - …
- The role of plasma oscillations on propulsive performances and transport is recently gaining interest
  - One well known example is anomalous transport in Hall Effect Thrusters

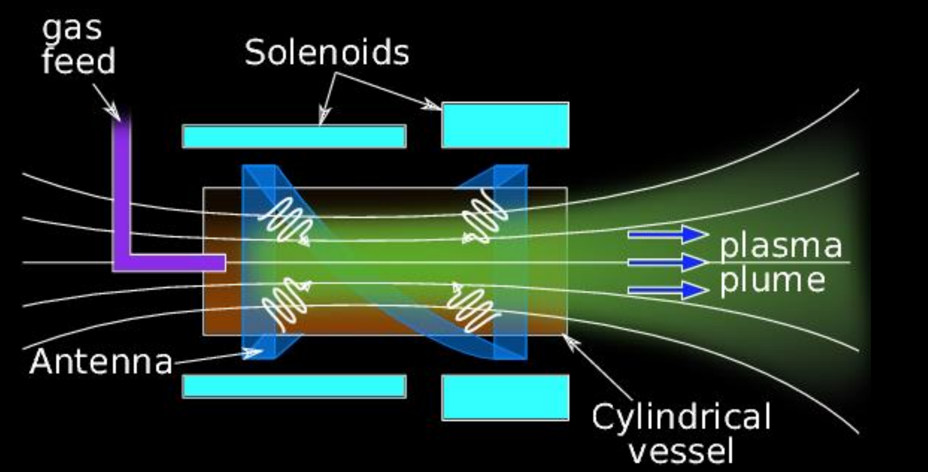

Schematics of a Helicon plasma thruster with magnetic nozzle

Experiment overview

- A setup of three non-compensated Langmuir probes was used to gather the data
- The probe tips are 10 mm apart
- The position of the probe system is moved remoted through a mechanical arm
- Reference case at 5 SCCM, 10 SCCM and 20 SCCM cases scanned with less positions
- Time-averaged measurements of I-V characteristics are used to characterize the plasma
- Time-resolved signals of two probes are cross-correlated in order to extract wave information

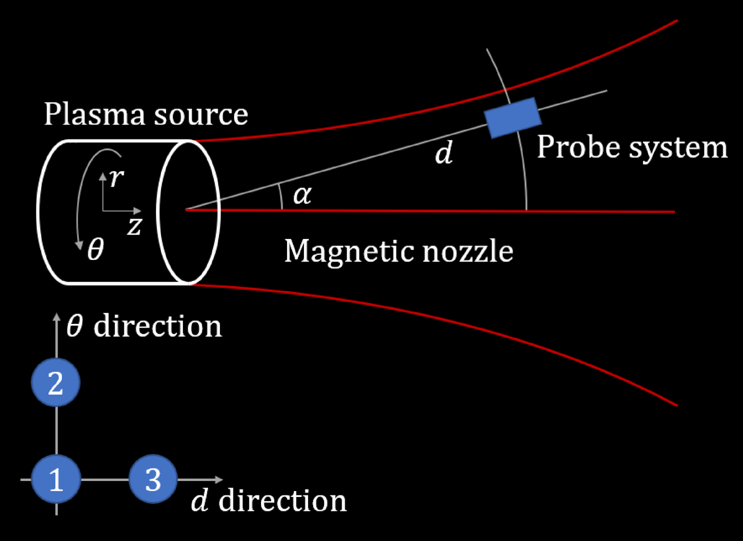

Overview of the Langmuir probe setup

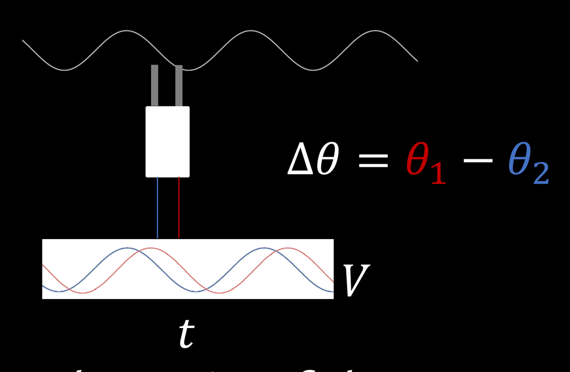

Schematics of the wave-probe interaction

Description of the statistical tools employed

- By using a pair of aligned probes, the dispersion diagram in one direction can be recovered (*PSD2P technique*)
  - Using additional probes allows to resolve multiple directions simultaneously
- If the probes are positioned at $x_1 = x_0$ and $x_2 = x_0 + \chi$, the cross correlation
$$H(\chi,\omega) = \hat{\varphi}(x_0,\omega)\hat{\varphi}^*(x_0+\chi,\omega) = \mathrm{Re}\{H\} + i\mathrm{Im}\{H\}$$
Provides with the *local wavenumber*
$$K(\omega) = \tan^{-1}[\mathrm{Im}\{H\}/\mathrm{Re}\{H\}]/\chi$$
and the *cross-power magnitude*
$$\rho(\omega) = |H(\chi,\omega)|$$
- The bivariate sample cross spectrum is defined as
$$H(k,\omega) = I_{[0,\Delta k)}(k - K(\omega)) \times \rho(\omega)$$
- *Mean* and *standard deviation* of both local wavenumber and cross-power magnitude are computed
  - The local wavenumber is treated with a circular normal distribution
  - The cross-power magnitude is treated with a log-normal
- *Mean standard coherence (MSC)* is also employed

Oscillation overview

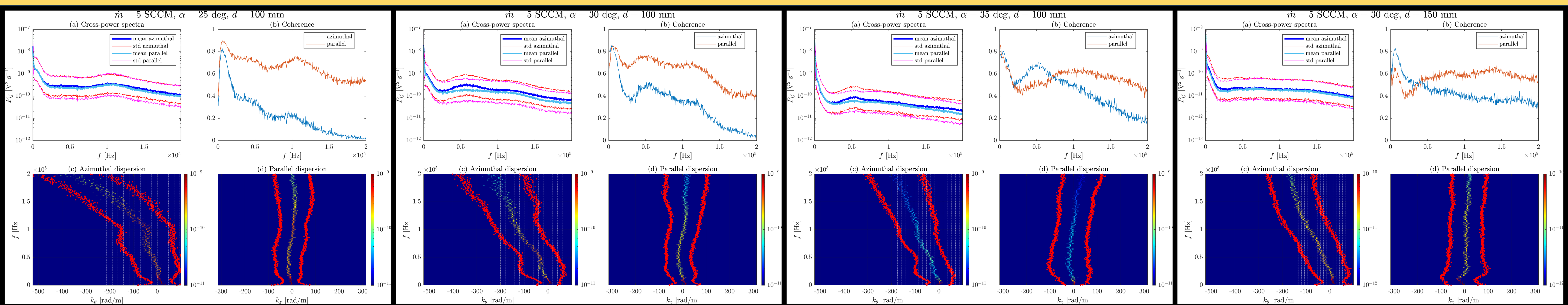

Dispersion diagrams, power and coherence plots obtained through cross-correlation

- A broadband azimuthal oscillation in the negative θ direction (diamagnetic) is visible far from the nozzle and away from the centreline
  - Both for $d = 100$ mm and $d = 150$ mm but not at $d = 50$ mm
  - It begins developing only at α = 15-20 deg, depending on the distance
  - It stays clearly visible until $\alpha = 35$ deg
- If the mass flow rate is increased at 10 SCCM, the results become more ambiguous and the power decreases
  - The negative trend in the azimuthal direction persists, even though less clearly
  - The same broadband oscillation is still visible at some (less) positions
- At 20 SCCM, the power keeps decreasing and the oscillations are not visible any longer
- The oscillation extends up until several hundreds of kHz
- Some positions (low α) for $d = 100$ show a change of behavior around 100 kHz
  - At $\alpha = 25$ deg, a power concentration corresponds to that frequency
- At $d = 100$ mm, the azimuthal coherence grows overall by increasing α
- Positions $\alpha = 30$ and 35 deg show no change in behavior, with power concentrations around 50 kHz, for m = 1-2
  - The power concentration is stronger in the azimuthal direction
  - For this frequency, the coherence peaks
  - The 100 kHz behavior is mildly still visible at $\alpha = 30$ deg, but disappears at $\alpha = 35$ deg
- At $d = 150$ mm there is no power concentration visible
- Similarly happens for increased mass flow rate $\dot{m} = 10$ SCCM (not shown)

Discussion of the results

- The phase velocities computed at 50 and 100 kHz are in the 10^3- 10^4 m/s range, depending on the position
- The ExB and diamagnetic drifts are opposite in sign throughout most of the plume except for some low α at higher distances
  - This does not meet the Simon-Hoh fluid instability condition [1]
- Both drifts fall in the 10^5 m/s
  - The ballistic mode is therefore not a good candidate [2]
- Experimental evidence of similar oscillations in recent literature propose other explanation, namely the magnetosonic wave [3] and the lower-hybrid-drift instability (LHDI) [4]
  - The magnetosonic wave scales with the Alfvén velocity though, which falls in the range of 10^5 m/s, making it not a good candidate
  - The LHDI, instead, scales with $\rho_L\omega_{LH}$ when its growth rate is maximum, which takes place for $k_\parallel = 0$ [5]
    - The LHDI quasi-neutral fluid limit however returns the Simon-Hoh

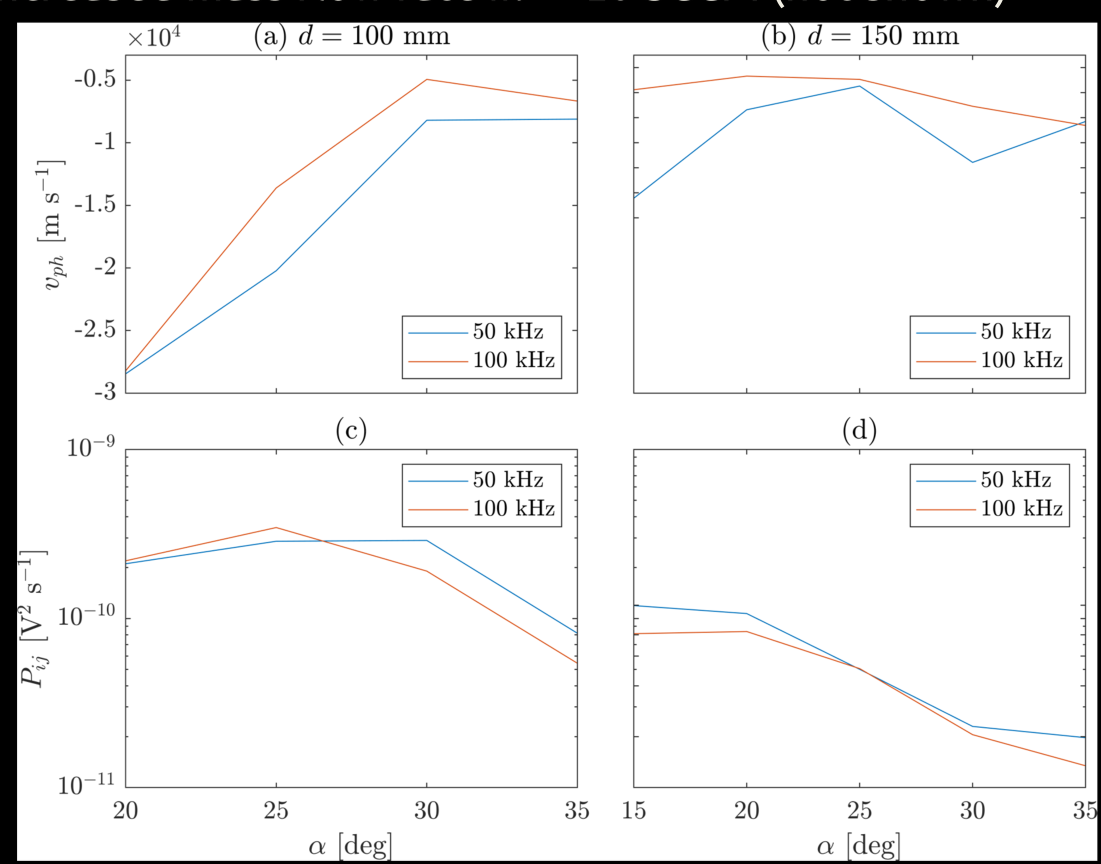

Evolution of phase velocity and power around 50 and 100 kHz along α

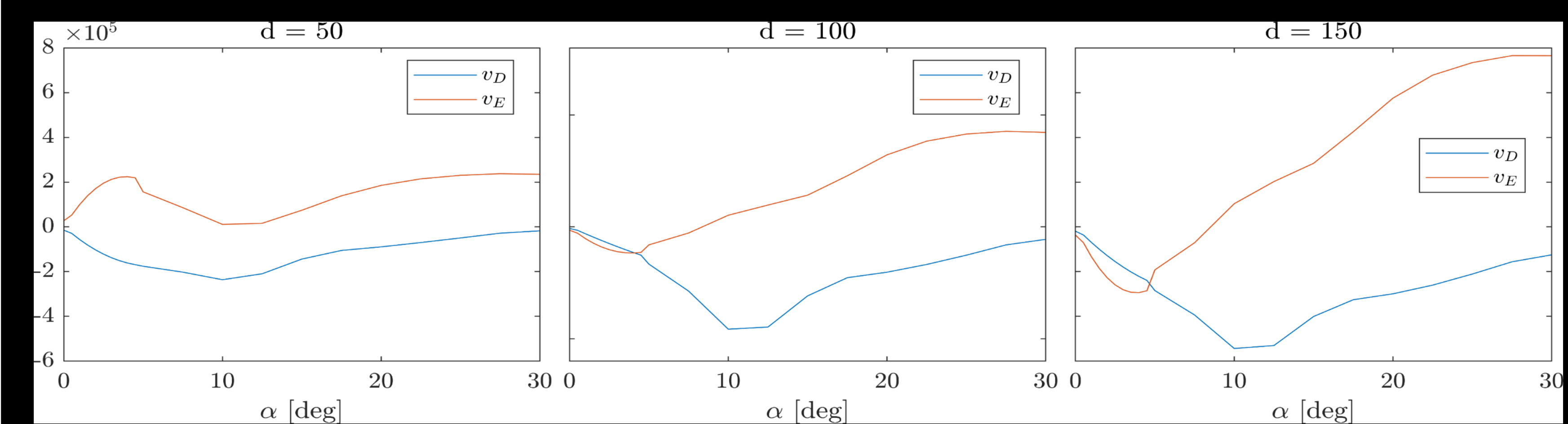

Evolution of ExB and diamagnetic drifts along α

ω/ω_{LH}	$k\rho_L$	$v_{ph}/\rho_L\omega_{LH}$
$0.31 - 1.67$	$0.15 - 0.70$	$1.65 - 6.60$
ω_{LH} [Hz]	ρ_L [m]	$\rho_L\omega_{LH}$ [m s^{-1}]
$60 - 160 \times 10^3$	$3 - 7.5 \times 10^{-3}$	3.03×10^3
v_A [m s^{-1}]	ω_{pe}/ω_{ce}	ω_{pi}/ω_{ci}
$0.42–2.42 \times 10^5$	$2.54 - 31.3$	$0.12 - 1.53 \times 10^4$

Acknowledgments

This project has received funding from the European Research Council (ERC) under the European Union's Horizon 2020 research and innovation programme (grant agreement No 950466)

References

[1] Smolyakov, A. I., et al. "Fluid theory and simulations of instabilities, turbulent transport and coherent structures in partially-magnetized plasmas of discharges." Plasma Physics and Controlled Fusion 59.1 (2016): 014041.

[2] Swanson, D.G. Plasma Waves, 2nd Edition. IOP Publishing, Bristol, UK, 2003.

[3] Takahashi, K., Christine, C., and Boswell, R. W. "Wave-driven electron inward transport in a magnetic nozzle." Scientific reports 12.1 (2022): 20137.

[4] Hepner, S., Wachs, B., and Jorns, B. "Wave-driven non-classical electron transport in a low temperature magnetically expanding plasma." Applied Physics Letters 116.26 (2020): 263502.

[5] Carter, T. A., et al. "Experimental study of lower-hybrid drift turbulence in a reconnecting current sheet." Physics of Plasmas 9.8 (2002): 3272-3288.